Counterintuitive effects of isotopic doping on the phase diagram of H_2–HD–D_2 molecular alloy

Xiao-Di Liu[a,1], Philip Dalladay-Simpson[b], Ross T. Howie[b], Hui-Chao Zhang[a,c], Wan Xu[a,c], Jack Binns[b,2], Graeme J. Ackland[d,e], Ho-Kwang Mao[b,1], and Eugene Gregoryanz[a,b,d,e,1]

[a]Key Laboratory of Materials Physics, Institute of Solid State Physics, Chinese Academy of Sciences, Hefei 230031, China; [b]Center for High Pressure Science & Technology Advanced Research, Shanghai 201203, China; [c]University of Science and Technology of China, Hefei 230026, China; [d]Centre for Science at Extreme Conditions, University of Edinburgh, Edinburgh EH9 3FD, United Kingdom; and [e]School of Physics and Astronomy, University of Edinburgh, Edinburgh EH9 3FD, United Kingdom

Contributed by Ho-Kwang Mao, April 9, 2020 (sent for review January 21, 2020; reviewed by Yuichi Akahama and Sandro Scandolo)

Molecular hydrogen forms the archetypical quantum solid. Its quantum nature is revealed by behavior which is classically impossible and by very strong isotope effects. Isotope effects between H_2, D_2, and HD molecules come from mass difference and the different quantum exchange effects: fermionic H_2 molecules have antisymmetric wavefunctions, while bosonic D_2 molecules have symmetric wavefunctions, and HD molecules have no exchange symmetry. To investigate how the phase diagram depends on quantum-nuclear effects, we use high-pressure and low-temperature in situ Raman spectroscopy to map out the phase diagrams of H_2–HD–D_2 with various isotope concentrations over a wide pressure–temperature (*P-T*) range. We find that mixtures of H_2, HD, and D_2 behave as an isotopic molecular alloy (ideal solution) and exhibit symmetry-breaking phase transitions between phases I and II and phase III. Surprisingly, all transitions occur at higher pressures for the alloys than either pure H_2 or D_2. This runs counter to any quantum effects based on isotope mass but can be explained by quantum trapping of high-kinetic energy states by the exchange interaction.

hydrogen | deuterium | high pressure

Hydrogen and deuterium have unique and distinctive properties which set them aside from the rest of the periodic table. Hydrogen has the lowest nuclear mass, and H_2:D_2 has the highest isotope mass ratio of any element 1:2 (1). Consequently, quantum effects such as zero-point energy are both large and different for the two isotopes. This energy, combined with the effects of exchange symmetry, via the *ortho*–*para* (*o-p*) distinction, results in fascinating behavior at low temperatures (2).

It is believed that the molecular hydrogens form the same series of phases if pressurized and/or cooled, although with measurably different phase boundaries. There are five experimentally described solid molecular phases in the pure isotopes (2–12). In a qualitative description (13), phase I adopts a hexagonal close-packed arrangement of rotating molecules. Rotation at very low temperature is only possible due to quantum nuclear effects for which the rotational ground state has no zero-point energy. Phases II and III are typical molecular phases (2, 8), where symmetry breaking arises from quadrupole–quadrupole interactions [phase II (14)] or efficient packing of elongated molecules [phase III (13)]. Phases IV and V possess mixed molecular states with both strongly bound rotating and weakly bound molecules (4, 5, 15). The phase I(II)→III transition is density driven, resulting in a close to vertical phase line (quasi-isobaric) separating the two phases (2, 16, 17). Conversely, the I→II and III→IV(V) transformations are mostly temperature (entropy) driven, resulting in a flatter phase line (quasi-isothermal) separating the partially ordered phase II from the rotor phase I and the mixed-molecular phases IV(V) from phase III (4, 18). The situation is further complicated by the *o-p* distinction: due to the exchange symmetry, *ortho*-H_2 (o-H_2) is unable to be in the $J = 0$ molecular rotational ground state. This means that phase I of o-H_2 has higher energy than phase I of *para*-H_2 (p-H_2), and therefore, o-H_2 transforms more easily to phase II than p-H_2 (*SI Appendix*, Fig. S1).

Hydrogen deuteride has been studied less than the pure isotopes, and its spectroscopy is complicated by the localization of the vibrational modes. Pure HD was claimed to have a phase II with an unusual reentrant phase line at low temperatures (19, 20), and on further compression above ∼160 GPa, to transform to phase III (21). Recently, using Raman spectroscopy, phase IV was found in H_2, HD, and D_2 mixtures at 300 K (1). A subsequent infrared study of pure HD speculated to observe dissociation at 77 K, and at pressures above 160 GPa, suggested the existence of two novel phases (HD-IV* and HD-PRE) (22), which do not exist in pure isotopes.

Recently, we reported the behavior of the pure isotopes at low temperatures up to pressures of 210 GPa, characterizing the phase transition criteria between phases I, II, and III. These measurements suggested the existence of a phase II' in D_2 which is not observed in H_2 (2, 23). We speculated that its presence is related to the lower zero-point energy of D_2 compared to H_2 and more complex rotational movement (2). The presence of both isotopes, H and D, makes only a subtle difference to the electronic structure, but the disorder can fundamentally change vibrational properties from its pure counterparts. In an HD molecule, the nuclei are distinguishable, so

Significance

When hydrogen and deuterium are mixed, they form H_2 + HD + D_2 mixtures at very low pressures and room temperature. We show that at high pressures and low temperatures these mixtures behave as an isotopic molecular alloy (ideal solution); exhibiting symmetry-breaking phase transitions between phases I, II, and III; and shifting the transformations to phases II and III to higher pressures as compared to pure isotopes. This runs counter to any quantum effects based on isotope mass but can be explained by quantum trapping of high-kinetic energy states by the exchange interaction.

Author contributions: X.-D.L. and E.G. designed research; X.-D.L., P.D.-S., R.T.H., H.-C.Z., W.X., J.B., and E.G. performed research; X.-D.L., P.D.-S., R.T.H., H.-K.M., and E.G. contributed new reagents/analytic tools; X.-D.L., P.D.-S., R.T.H., G.J.A., and E.G. analyzed data; H.-K.M. contributed to the discussion of results; and X.-D.L., G.J.A., and E.G. wrote the paper.

Reviewers: Y.A., University of Hyogo; and S.S., The Abdus Salam International Center for Theoretical Physics.

The authors declare no competing interest.

[1]To whom correspondence may be addressed. Email: xiaodi@issp.ac.cn, maohk@hpstar.ac.cn, or e.gregoryanz@ed.ac.uk.

[2]Present address: School of Science, RMIT University, Melbourne, Victoria 3000, Australia.

This article contains supporting information online at https://www.pnas.org/lookup/suppl/doi:10.1073/pnas.2001128117/-/DCSupplemental.

there is no *o-p* distinction, allowing all angular momentum states ($J = 0, 1, 2, \ldots$). Additionally, HD molecules possess a small permanent dipole moment (5.85×10^{-4} D) as well as the center of mass being off center. All of these, together with the random distribution of the isotopes in the solid (1), might significantly affect the formation of phase II. Such effects raise important questions about how isotopic mixtures behave: how do the quantum effects due to mass and to *o-p* symmetry compete; would the isotopes separate, and if not, would the isotopic disorder play any role in packing of the molecules; could new phases exist; will each species break symmetry at the same pressure–temperature (P-T) conditions; and how might isotopic doping alter the phase boundary?

Here we study compressed hydrogen–deuterium mixtures at low temperatures. Remarkably, we find that the mixtures have a higher transformation pressure (equivalently, lower temperatures) to phases II and III than either H_2 and D_2. For example, at 20 K, the mixtures enter phase II above 65 GPa and phase III above 170 GPa depending on concentration, while for n-D_2 (H_2) these pressures are $\sim$20 GPa [$\sim$60 GPa (2, 24)] for phase II and 165 (160) GPa for phase III (2). Since HD has mass intermediate between H_2 and D_2, this cannot be due to mass effects alone.

We studied three concentrations of mixtures: H:D = 40:60 (D_2-rich), H:D = 50:50, and H:D = 75:25 (H_2-rich). Upon loading the mixtures of H_2 and D_2 at 0.2 GPa, we observe the formation of HD within minutes at 300 K. Assuming the reaction $H_2 + D_2 \leftrightarrow HD$ is completely reversible, the following molecular isotopic alloys are formed from the initial concentrations: 40:60, $(H_2)_{0.16}(HD)_{0.48}(D_2)_{0.36}$; 50:50, $(H_2)_{0.25}(HD)_{0.5}(D_2)_{0.25}$; and 75:25, $(H_2)_{0.56}(HD)_{0.38}(D_2)_{0.06}$, reflecting the overall intensity distribution at low pressures (1) (*SI Appendix*, Figs. S2 and S3). This results in mixtures that have comparable HD concentrations, varying by a maximum of 12%, whereas the D_2 concentration varies from 6 to 36%.

Measurements were conducted through both isobaric cooling/heating cycles and isothermal compressions at low temperature (Fig. 1). We identify the phase changes using standard phase transformation criteria (2), namely, the appearance of new, sharp, low-frequency excitations and changes in the pressure/temperature dependence of the vibron frequencies.

Fig. 2 shows a representative temperature scan of the 75:25 mixture at 116 GPa. As the temperature is decreased below 75 K, both criteria are clearly observed in the Raman spectra: the appearance of new peaks (Fig. 2, *Left*) and a change in temperature dependence of the vibrational frequencies (Fig. 2, *Right*). It is significant that the changes in the frequencies of the H–H and H–D vibrons vs. temperature happen simultaneously and have the same shapes as observed in pure D_2 and H_2 at similar pressures (2). At this particular concentration, we also observe noticeable asymmetric broadening of all stretching modes, with the D–D appearing as a doublet in phase I (Fig. 2, *Middle*), and on the transition to phase II, a 3rd peak can be resolved at the same temperature as the change of vibrational frequency temperature dependency of the H–H and H–D modes (Fig. 2 and *SI Appendix*, Figs. S4 and S5). The asymmetric broadening of the Raman modes in mixtures at 300 K was reported before, but no splitting was observed (1). The splitting (less resolved but still present for H–D and H–H modes) could be explained by the mode localization arising from the different atomic environment (25). In all of the three concentrations studied, changes to H_2, D_2, or HD modes happen simultaneously, showing that the mixtures behave as a molecular alloy (*SI Appendix*, Figs. S5–S7). It is interesting to note that we have not observed spectra similar to those of phase II in pure HD (19).

Figs. 3 and 4 show the evolution of the low-frequency (librons) and vibrational parts (vibrons) of the Raman spectrum of three mixtures during the isothermal compression in the 7 to 200 GPa pressure regime. At low pressures, i.e., 7 to 20 GPa, the rotational part of the spectra could be described as the linear superposition of three independent isotopic molecules, although the rotational modes of HD are considerably broader than those of D_2 and H_2 (see *SI Appendix*, Fig. S3, and also ref. 1). We propose that the broadening can be understood by the offset of the center of mass: as the HD molecule rotates, its charge density wobbles much more than H_2, facilitating collisions with adjacent molecules. This reduces the rotational mode lifetime and increases the HD rotor line width.

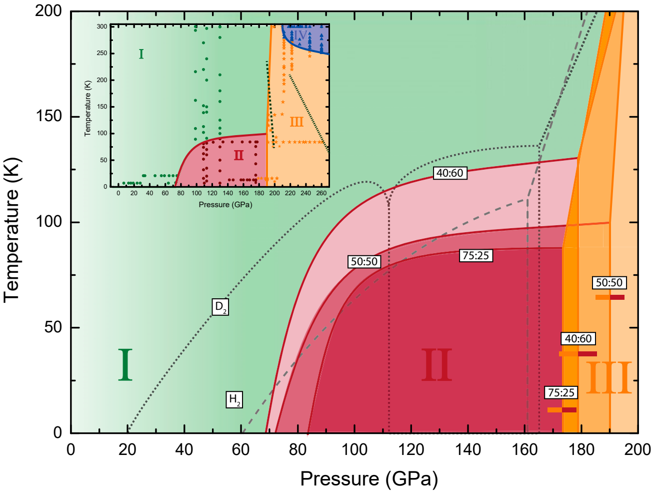

Fig. 1. The proposed low-temperature phase diagrams of three representative H_2–D_2 mixtures (H_2:D_2 ratios of 75:25 = 3:1, 50:50 = 1:1, and 40:60 = 2:3). Phase I is shown in green, phase II is shown in red, and phase III is shown in orange. Different shades of color in phase II and phase III represent different mixture concentrations. The gray dashed lines represent the phase boundaries of the pure isotopes taken from ref. 2. (*Inset*) Extended phase diagram of the individual 50:50 mixture, showing collected data points on isothermal compression and isobaric cooling cycles. Phase IV is shown in blue. Green dashed lines represent previously proposed boundaries from ref. 22. We see no evidence for reentrant phase boundaries down to 13 K.

The vibrational modes can be assigned to three types of molecules; however, their frequencies are all higher in mixtures than in the pure isotopes (*SI Appendix*, Fig. S12). This is due to resonant coupling between the vibrations on identical molecules. In mixtures, most neighbors are of a different species; hence, there is vibrational decoupling, and the modes are more localized. The coupling has two effects: it shifts the mean frequency downward and creates dispersion. Since the Raman active mode has typically the lowest frequency in the phonon band, the dispersion lowers the Raman frequency further. By contrast, the IR active modes are nearer to the top of the band, so in IR the two effects tend to cancel out. In fact, the Raman vibrational frequencies of H–H, H–D, and D–D modes in mixtures are located at the range between Raman and infrared frequencies in the pure isotopes, as shown in *SI Appendix*, Fig. S13. This also shows the comparison of Raman vibrational frequencies of H–H mode calculated in the ideal mixing of the alloy and measured in our experiment with different concentrations.

There is an interesting feature shared by all concentrations: rapid decrease of the H_2 vibron intensity as pressure is increased (Fig. 4). While the vibrational modes attributed to D_2 and HD increase in intensity, the modes corresponding to hydrogen become significantly broader. This phenomenon was observed at room temperature and can be explained by H_2 being the lightest molecule, and therefore, it is scattered the most in collision with other molecules (1). Due to this effect, at pressures above 50 to 60 GPa, the overall appearance of the rotational/librational part of the Raman spectra is closer to pure D_2 (even for the 50:50 mixture at high pressures), while the spectra of the 40:60

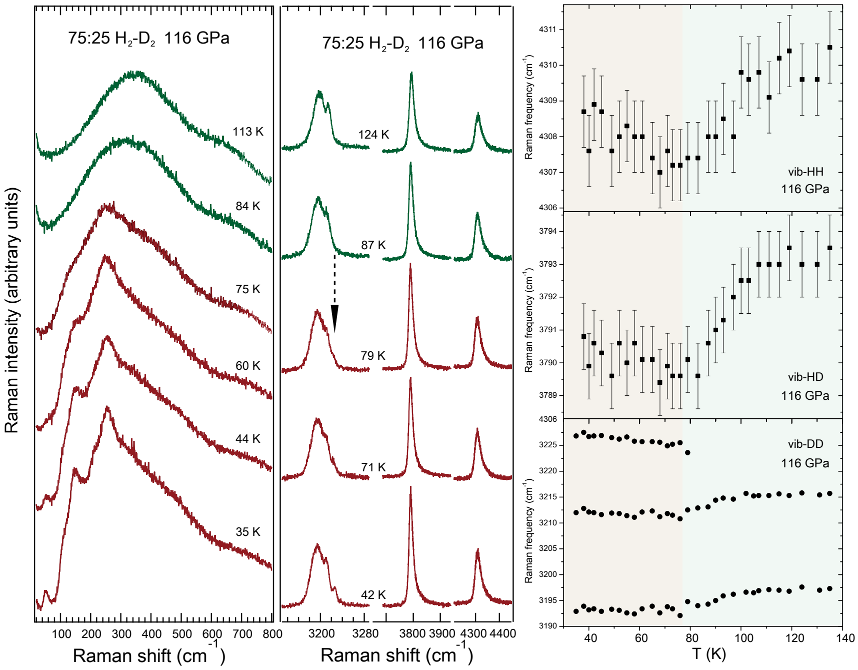

Fig. 2. (*Left* and *Middle*) Representative rotational, librational, and vibrational Raman spectra of a 75:25 H_2–D_2 mixture as a function of temperature at 116 GPa. Arrow indicates of the appearance of a new vibrational mode at the transition to phase II. The D–D peak is nearly as wide as the others: note the change in scale on the x axis. (*Right*) Vibron frequencies of H–H (*Top*), H–D (*Middle*), and D–D (*Bottom*) as a function of temperature at 116 GPa for the same mixture concentration. The error bars are the fitting error of the position of vibron frequencies. Colors indicate phase I (green) and phase II (red).

mixture are almost indistinguishable from those of pure D_2 (figures 3 and 1 in ref. 2). As pressure is increased above 60 to 70 GPa, the librational modes broaden and overlap significantly, making assignment difficult, with only the predominant $S_0(0)$ modes in D_2 or H_2 clearly resolvable at around 200 cm^{-1} at 65 GPa for the 40:60 mixture and around 360 cm^{-1} at 76 GPa for the 75:25 mixture. Interestingly, the same modes are also relatively well defined in 50:50 mixture at 74 GPa even though the HD–$S_0(0)$ was the predominant excitation at 29 GPa (Fig. 3, *Middle*).

When pressures above 100 GPa are reached, sharp low-frequency peaks emerge (Fig. 3; see 95, 110, and 105 GPa), and the spectra of the 40:60 and 50:50 concentrations start to closely resemble those of pure D_2 in phase II (2), while the 75:25 spectra appear broadly similar to those of pure hydrogen (2) (Fig. 3 and *SI Appendix*, Figs. S6–S8). However, the transformation to phase II happens in the alloy at 69 GPa for 40:60, 75 GPa for 50:50, and 84 GPa for the 75:25 alloy (mixture) (Figs. 1 and 3). The transformation pressures (at similar temperatures) to phase II depend on o-p ratio: for n-D_2 (*normal*-D_2, 2/3 *ortho*, and 1/3 *para* mixed state) and o-D_2 vary from around 20 to 25 GPa (6, 24) and from 60 to 110 GPa for n- and p-H_2 (2, 26), while for pure HD, the transformation pressure is around 60 GPa (21). The most unusual observation here is that even in the mixture (40:60), the Raman spectra look almost identical to those of pure D_2 (Fig. 3, *Left* and *SI Appendix*, Figs. S9 and S10). However, the transition pressure to phase II is about 69 GPa, which is almost a threefold increase compared with pure D_2. In fact, the presence of hydrogen in the alloy pushes the phase II boundary of all concentrations close to that of pure p-H_2 at around 110 GPa (26).

The pressure needed to transform pure p-H_2 (sample was keeping at 30 K for 72 h to achieve complete conversion) to phase II (∼110 GPa) (26) is higher than that in the mixed o-p equilibrium state (∼60 GPa) (on the time scale of our experiment, ∼3 to 5 h) (2). This is primarily because the o-H_2 molecules in phase I are required by exchange symmetry to be in the $J=1$ rotational state; this trapped kinetic energy makes them less stable than the ground $J=0$ state adopted by p-H_2. One can expect the same destabilization of phase I to apply p-D_2. However, because the excess energy of the $J=1$ state is lower, and the $J=1$ fraction at high-T is also lower (nuclear spin-state degeneracy of 3:6 rather than 3:1), the destabilization of D_2 phase I is much smaller.

One might expect isotopic mixtures to be intermediate between H_2 and D_2, but in fact, this scenario plays out in a more counterintuitive way at very low T when the o–p ratio is trapped

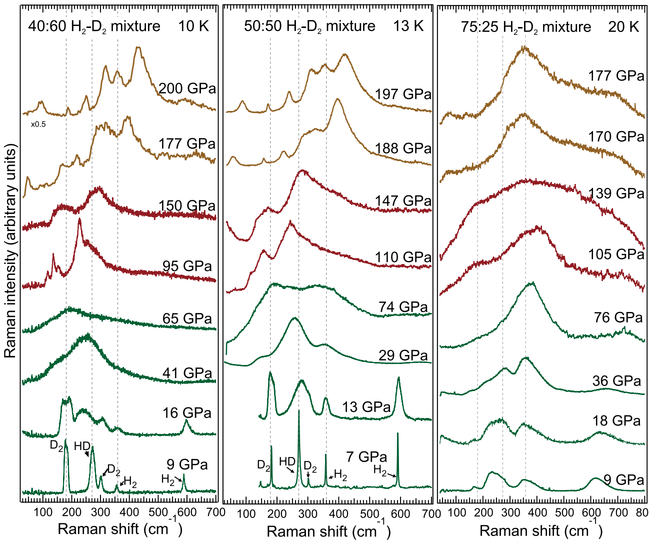

Fig. 3. Representative low-frequency Raman spectra of (*Left*) 40:60, (*Middle*) 50:50, and (*Right*) 75:25 H_2–D_2 mixtures as a function of pressure at 10, 13, and 20 K respectively. Colors indicate phase I (green), phase II (red), and phase III (orange).

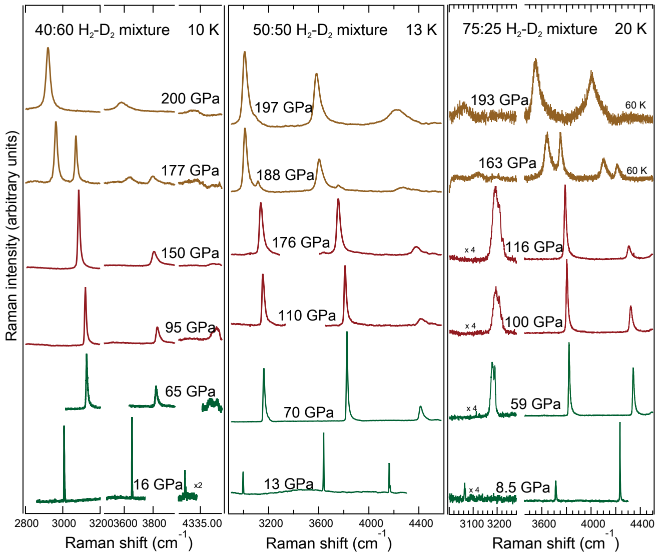

Fig. 4. Representative vibrational Raman spectra of (*Left*) 40:60, (*Middle*) 50:50, and (*Right*) 75:25 H_2–D_2 mixtures as a function of pressure at 10, 13, and 20 K, respectively. Colors indicate phase I (green), phase II (red), and phase III (orange).

at its room temperature equilibrium value. This is due to the effect we call quantum trapping.* Direct evidence of quantum trapping is clearly shown in Fig. 3 where the S(1) Raman transition (due to the trapped $J = 1$ states) is observed for H_2 or D_2 but absent for HD. To our knowledge, this is the only qualitative experimental signature of the exchange interaction. As seen in Fig. 3, the broken-symmetry phase II is characterized by nonrotor peaks around 150 cm^{-1}.

The trapped kinetic energy in $J = 1$ states increases the free energy of phase I (*SI Appendix*, Fig. S1). However, since HD molecules have no exchange symmetry, at low temperature all HD molecules will be in the $J = 0$ ground state, so the trapped kinetic energy of phase I is lower in mixtures than in either pure element. Consequently, phase I survives to higher pressures in the molecular alloy. Of course, the zero-point effects are still smaller in HD than in H_2, so the HD transition still occurs at lower pressure than in $para$-H_2. The exact position of the transition will depend on both the H:D concentration and the o-p ratio.

Fig. 4 shows isotope effects in the transition to phase III: mixtures transform at higher pressures than the pure species. The transition to phase III is characterized by the splitting of the ν_1 modes, identical to that observed in the pure isotopes. As with the phase I to II transition, the mixtures are behaving like a molecular alloy, with all peaks splitting simultaneously from phase II to phase III. At low temperatures (around 20 K) the II to III phase transition starts at approximately 160, 159, and 165 GPa (2, 21) for pure H_2, HD, and D_2, respectively, while phase III occurs at 177, 185, and 171 GPa for the 40:60, 50:50, and 75:25 alloys (Fig. 4). Similar to the pure isotopes, all three mixture concentrations have phase coexistence regimes of approximately 10 to 15 GPa.

The phase II to III transition occurs at pressures where the vibron frequency is significantly decreasing, presumably associated with increased bond length and the molecule becoming more elliptical. Thus, the packing efficiency of three-dimensional ellipsoids can be taken as the driving force for the transition (13). The electric dipole of HD is so small that dipole–dipole interactions contribute only μeV of energy. It is well known that polydispersity reduces the packing efficiency, so the thermodynamic density advantage of phase III is lower in mixtures, meaning that higher pressures are required to stabilize it.

By combining all of the P-T paths taken for the different concentrations, we are able to constrain the phase diagram of the H–D molecular alloys (Fig. 1) with o-p ratios characteristic of rapid cooling. Although the overall phase diagram(s) resemble the pure isotopes, there are some interesting and unusual features. All of the phase I to II transition pressures in mixtures of all concentrations are higher than those of pure isotopes. Logically, the phase boundaries of the mixtures is consistent with that of the predominant isotope; i.e., the 40:60 mixture boundary is at lowest pressure which is closest to that of pure D_2 among these three concentration mixtures, while 75:25 mixture boundary is at the highest pressure which closest to that of pure H_2 among these three concentration mixtures. We note here that the Raman spectra in phase II could also be described as either hydrogen-like, having features similar to pure hydrogen (Fig. 3 and *SI Appendix*, Fig. S11, 75:25 mixture), or deuterium-like, having features similar to pure deuterium (Fig. 3 and *SI Appendix*, Fig. S11, 40:60 mixture and 50:50 mixture).

Surprisingly, the mixtures' phase II to III transition boundaries do not lie between those of hydrogen and deuterium as one would expect but are shifted to higher pressures starting the transition at 163 GPa and completed by 191 GPa (*SI Appendix*, Fig. S12). Just like in case of phase I to phase II the doping stabilizes the lower-pressure phase (phase II in this case). It is interesting that phase II of the 50:50 molecular alloy appears to resist the transformation to phase III up to the highest pressures and covers a larger amount of P-T space.

We have also explored the phase III to IV boundary in the molecular alloys. The Raman spectra of the 50:50 mixture collected over a broad region of phase III (see the P-T paths taken in Fig. 1, *Inset*) indicate that phase III is stable up to 260 GPa in a broad temperature range, transforming to phase IV at temperatures above ~250 K. A recent IR study (22) showed that above 160 GPa, pure HD dissociates and recombines forming a molecular mixture of H_2, HD, and D_2 similar to the 50:50 mixture studied here. It was then claimed that this mixture forms two novel phases, above 200 GPa, IV* and HD-PRE, both of which occupy phase space that we attribute to phase III (see phase lines in Fig. 1, *Inset*). Our current study, and a previous room temperature study (1), suggests that the overall appearance of the phase diagrams of the molecular alloys is similar to those of the pure elements. Ref. 22 presented only one experimental run, without any raw data present, making it unclear what exactly their transition criteria to these phases are. It is also peculiar that these transition lines do not resemble anything observed in the pure isotopes H_2 and D_2. Therefore, it is highly unlikely that the H:D mixture would have two solid phases never observed in pure hydrogen and deuterium.

The strong S(1) peaks seen after rapid cooling prove that the nuclear spin state is trapped. In the case of H_2 and D_2, the constraints from exchange symmetry mean some molecules are trapped in the high-energy $J = 1$ rotational state in phase I. This extra rotational energy destabilizes phase I with respect to phase II, causing the transition to occur at lower pressures than in HD-containing mixtures. This quantum trapping of rotational energy has the effect of moving the phase boundaries in a reproducible manner.

Methods

Samples of H_2–D_2 mixtures were produced by combining research-grade (99.999% purity) H_2 and D_2 in the gas phase (typically <10 MPa) at 300 K. The partial pressures of each species were then used to calculate the

---

*Details of the *para* and *ortho* states and corresponding statistics are given in *SI Appendix*.

compositions. Immediately after loading at 0.2 GPa, the Raman modes of H_2 and D_2 are clearly observed while the Raman mode corresponding to HD is weak, suggesting the dissociation and recombination of the molecules at this density is kinetically slow. Upon further compression in the fluid state (>0.5 GPa), HD begins to rapidly form, evident through the H–D vibrational mode which grows with intensity with time until equilibrium is reached between H_2, HD, and D_2. After the equilibrium is reached the intensities of three vibrational modes in the fluid state correspond to the gas concentration (see *SI Appendix* for more details and calculations) and do not change with time implying the reversibility of the reaction.

Raman spectroscopy measurements were made using a custom-built microfocused Raman system (2). The excitation source was a 532-nm laser, and the laser power was between 10 and 50 mW, with collection times ranging between 3 and 30 s. For diamonds with culet size bigger than 100 μm and pressure below 50 GPa, the pressure was measured using ruby spheres and correlated with the frequency of the stressed diamond edge. For diamond with culet size smaller than 100 μm or pressure above 50 GPa the stressed diamond edge was used to estimate the pressure using the relationship from Akahama and Kawamura (27).

In the typical isothermal experiment the sample was cooled down within 1 to 2 h and then the Raman spectra were collected within 3 to 4 h upon pressure increase. In the typical isobaric experiment the target pressure would be reached at 300 K, the sample cooled within 1 to 2 h, and Raman spectra were measured upon warming. In our experiments the samples were not kept at very low temperatures (<50 K) for more than 5 to 6 h (see ref. 24 where normal hydrogen [deuterium] converted to the *p*-H_2 [*o*-D_2] after approximately 3 d at below 50 K). For examples, the estimate of the intensities of the $S_0(0)$ and $S_0(1)$ at 0.5 to 1 GPa and 300 K gives expected *o*-*p* ratio of 3:1 for H_2 and 2:3 for D_2. Upon cooling to 20 K, which usually takes around 3 h, at pressures below 50 GPa the ratio hardly changes for H_2. Therefore, we consider our sample to be in the mixed *ortho*–*para* state. All data referred to in the manuscript are available in the article and *SI Appendix*.

ACKNOWLEDGMENTS. This work was supported by research grants of National Science Foundation of China (11874361, 11404343, 51672279, 51727806, and 11774354), Chinese Academy of Sciences Innovation Fund (CXJJ-19-B08), Science Challenge Project (TZ201601), the Hefei Institutes of Physical Science Chinese Academy of Sciences Director's Fund (YZJJ201705), and the European Research Council (Hecate).

1. R. T. Howie, I. B. Magdău, A. F. Goncharov, G. J. Ackland, E. Gregoryanz, Phonon localization by mass disorder in dense hydrogen-deuterium binary alloy. *Phys. Rev. Lett.* **113**, 175501 (2014).
2. X. D. Liu, R. T. Howie, H. C. Zhang, X. J. Chen, E. Gregoryanz, High-pressure behavior of hydrogen and deuterium at low temperatures. *Phys. Rev. Lett.* **119**, 065301 (2017).
3. M. Eremets, Troyan, Conductive dense hydrogen. *Nat. Mater.* **10**, 927–931 (2011).
4. R. T. Howie, C. L. Guillaume, T. Scheler, A. F. Goncharov, E. Gregoryanz, Mixed molecular and atomic phase of dense hydrogen. *Phys. Rev. Lett.* **108**, 125501 (2012).
5. P. Dalladay-Simpson, R. T. Howie, E. Gregoryanz, Evidence for a new phase of dense hydrogen above 325 gigapascals. *Nature* **529**, 63–67 (2016).
6. I. F. Silvera, R. J. Wijngaarden, New low-temperature phase of molecular deuterium at ultrahigh pressure. *Phys. Rev. Lett.* **47**, 39–42 (1981).
7. I. Goncharenko, P. Loubeyre, Neutron and X-ray diffraction study of the broken symmetry phase transition in solid deuterium. *Nature* **435**, 1206–1209 (2005).
8. R. J. Hemley, H. K. Mao, Phase transition in solid molecular hydrogen at ultrahigh pressures. *Phys. Rev. Lett.* **61**, 857–860 (1988).
9. C. Zha, Z. Liu, M. Ahart, R. Boehler, R. J. Hemley, High-pressure measurements of hydrogen phase IV using synchrotron infrared spectroscopy. *Phys. Rev. Lett.* **110**, 217402 (2013).
10. H.-k. Mao, R. J. Hemley, Ultrahigh-pressure transitions in solid hydrogen. *Rev. Mod. Phys.* **66**, 671–692 (1994).
11. I. I. Mazin, R. J. Hemley, A. F. Goncharov, M. Hanfland, H.-k. Mao, Quantum and classical orientational ordering in solid hydrogen. *Phys. Rev. Lett.* **78**, 1066–1069 (1997).
12. G. Geneste, M. Torrent, F. Bottin, P. Loubeyre, Strong isotope effect in phase II of dense solid hydrogen and deuterium. *Phys. Rev. Lett.* **109**, 155303 (2012).
13. I. B. Magdău, M. Marqués, B. Borgulya, G. J. Ackland, Simple thermodynamic model for the hydrogen phase diagram. *Phys. Rev. B* **95**, 094107 (2017).
14. S. van de Bund, G. J. Ackland, Quadrupole arrangements and the ground state of solid hydrogen. *Phys. Rev. B* **101**, 014103 (2020).
15. H. Liu, L. Zhu, W. Cui, Y. Ma, Room-temperature structures of solid hydrogen at high pressures. *J. Chem. Phys.* **137**, 074501 (2012).
16. A. F. Goncharov, R. J. Hemley, H.-k. Mao, Vibron frequencies of solid H_2 and D_2 to 200 GPa and implications for the P–T phase diagram. *J. Chem. Phys.* **134**, 174501 (2011).
17. A. F. Goncharov, I. Mazin, J. H. Eggert, R. J. Hemley, H.-k. Mao, Invariant points and phase transitions in deuterium at megabar pressures. *Phys. Rev. Lett.* **75**, 2514–2517 (1995).
18. R. T. Howie, T. Scheler, C. L. Guillaume, E. Gregoryanz, Proton tunneling in phase IV of hydrogen and deuterium. *Phys. Rev. B* **86**, 214104 (2012).
19. F. Moshary, N. H. Chen, I. F. Silvera, Remarkable high pressure phase line of orientational order in solid hydrogen deuteride. *Phys. Rev. Lett.* **71**, 3814–3817 (1993).
20. Y. Crespo, A. Laio, G. E. Santoro, E. Tosatti, Theory of the reentrant quantum rotational phase transition in high-pressure HD. *Phys. Rev. B* **84**, 144119 (2011).
21. A. Chijioke, I. F. Silvera, Megabar-pressure infrared study of hydrogen deuteride. *Phys. Rev. Lett.* **97**, 255701 (2006).
22. R. P. Dias, O. Noked, I. F. Silvera, New phases and dissociation-recombination of hydrogen deuteride to 3.4 mbar. *Phys. Rev. Lett.* **116**, 145501 (2016)
23. X. D. Liu, R. T. Howie, H. C. Zhang, X. J. Chen, E. Gregoryanz, Liu et al. reply. *Phys. Rev. Lett.* **122**, 199602 (2019).
24. A. F. Goncharov, J. H. Eggert, I. I. Mazin, R. J. Hemley, H.-k. Mao, Raman excitations and orientational ordering in deuterium at high pressure. *Phys. Rev. B* **54**, R15590–R15593 (1996).
25. I. B. Magdău, G. J. Ackland, Infrared peak splitting from phonon localization in solid hydrogen. *Phys. Rev. Lett.* **118**, 145701 (2017).
26. H. E. Lorenzana, I. F. Silvera, K. A. Goettel, Orientational phase transitions in hydrogen at megabar pressures. *Phys. Rev. Lett.* **64**, 1939–1942 (1990).
27. Y. Akahama, H. Kawamura, Pressure calibration of diamond anvil Raman gauge to 310 GPa. *J. Appl. Phys.* **100**, 043516 (2006).